Evidence that hsp90 Is Involved in the Altered Interactions of *Acanthamoeba castellanii* Variants with Bacteria

Ling Yan,[1] Ronald L. Cerny,[2] and Jeffrey D. Cirillo[1]*

Departments of Veterinary and Biomedical Sciences[1] and Chemistry,[2] University of Nebraska, Lincoln, Lincoln, Nebraska 68583

There are many similarities between the interactions of environmental protozoa with pathogenic bacterial species and those observed in mammalian macrophages. Since single-celled protozoa predate mammalian hosts, it is likely that interactions in environmental biofilms have selected for many of the bacterial virulence mechanisms responsible for human disease. In order to better understand bacterial-phagocyte interactions, we developed a selection for *Acanthamoeba castellanii* variants that are more resistant to killing by bacterial pathogens. We identified four amoebal clones that display decreased phagocytosis of bacteria but no difference in uptake of latex beads compared to wild-type amoebae. These amoebal variants display differences in cellular morphology, partial resistance to killing by bacteria, more bactericidal activity, and higher frequencies of lysosome fusion with the bacterial vacuole. Three proteins are present at lower levels in these variants than in wild-type amoebae, and matrix-assisted laser desorption ionization–time of flight mass spectrometry allowed identification of two of them as actin and hsp90. We found that specific inhibitors of hsp90 produce a similar phenotypic effect in macrophages. These data suggest that hsp90 plays a role in phagocytic and, possibly, bactericidal pathways that affect interactions of phagocytic cells with bacteria.

Uptake and degradation of bacterial particles are key functions of phagocytes in the mammalian immune system. Phagocytic environmental protozoa within aquatic biofilms carry out analogous activities in complex ecosystems that contain numerous prokaryotic organisms. Recent data suggest that environmental protozoa, particularly amoebae such as *Acanthamoeba castellanii*, have played an important role in the evolution of bacterial pathogens of mammals and may represent natural hosts for virulent bacteria (4, 9). A number of different pathogenic species, including *Mycobacterium* spp. (12), *Vibrio cholerae* (69), *Burkholderia cepacia*, *Chlamydia pneumoniae*, *Edwardsiella tarda*, *Legionella pneumophila* (32, 59), *Cryptococcus neoformans* (66), *Listeria monocytogenes*, and *Francisella tularensis* (1), have the ability to survive and replicate in environmental protozoa. Environmental amoebae, including *A. castellanii*, can undergo a respiratory burst (19), produce oxygen radicals (20), express cell surface receptors (2), and have phagocytic mechanisms (3, 8, 39) that are similar to those of human macrophages.

There are several important steps during the interactions of phagocytic cells with bacterial pathogens, including adherence, phagocytosis, signal transduction, trafficking, and intracellular replication. It is likely that a large number of host cell components are involved in these processes, yet few have been described in great detail. Protozoal models for bacterial-host cell interactions, such as the amoeba *A. castellanii*, should be very useful for identification of the host cell components involved. As opposed to that of mammalian hosts, the unicellular nature of *A. castellanii* makes it possible to isolate clones for genetic analyses. Thus, the goal of the present study was to develop methods that would allow identification and characterization of host cell components involved in bacterial-host cell interactions in *A. castellanii*.

We developed a selection that would allow identification of amoebal variants having defects in pathways necessary for optimal host cell infection by using *L. pneumophila*, an intracellular pathogen that normally kills amoebae efficiently (11, 52). A total of four *A. castellanii* clones were isolated that display defects in their interactions with both mycobacteria and legionellae. These variants show decreased uptake of bacteria and enhanced bactericidal activity. Proteomic analyses suggest that decreased levels of hsp90 are responsible for the phenotype of the amoebal variants. In addition, pharmacological studies confirmed that inhibition of hsp90 in murine macrophages produces a similar phagocytic phenotype. Overall, these studies suggest, for the first time, that hsp90 is involved in phagocytosis of or bactericidal activity against bacteria in host cells.

MATERIALS AND METHODS

Cells and culture conditions. *A. castellanii* (ATCC 30234) amoebae, originally cultured from a single amoeba (47), were grown to 90% confluency at 23°C in the dark in 75-cm² tissue culture flasks (Falcon) in PYG broth (12). The amoebae were harvested before use by rapping the flask sharply to bring them into suspension, and the number of viable cells was determined as described previously (12). The MH-S (ATCC CRL-2019) murine alveolar macrophage cell line was maintained at 37°C and 5% CO_2 in RPMI 1640 medium with 2 mM L-glutamine (Gibco, Bethesda, Md.) supplemented with 10% heat-inactivated fetal bovine serum (Gibco), 10 mM HEPES, 1 mM sodium pyruvate, 4.5 g of glucose per liter, 1.5 g of bicarbonate per liter, and 0.05 mM 2-mercaptoethanol. The murine macrophage cell line J774A.1 (ATCC TIB67) was maintained at 37°C and 5% CO_2 in high-glucose Dulbecco's modified Eagle medium (Mediatech CELLGRO) supplemented with 10% heat-inactivated fetal bovine serum (Gibco) and 2 mM L-glutamine.

Bacterial strains and growth conditions. The *L. pneumophila* strain used for these studies, AA100, is a streptomycin-resistant variant (42) of *L. pneumophila* serogroup 1 (23). AA100 was grown on BCYE agar (22) for 3 days at 37°C in 5%

* Corresponding author. Mailing address: Department of Veterinary and Biomedical Sciences, University of Nebraska, Lincoln, 203 VBS, Fair and East Campus Loop, Lincoln, NE 68583. Phone: (402) 472-8587. Fax: (402) 472-9690. E-mail: jcirillo1@unl.edu.

CO_2 as described previously (10). Cultures of *M. marinum* strain M, a clinical isolate obtained from the skin of a patient (55), and *M. smegmatis* strain mc^{2}155 (63) were grown in Middlebrook 7H9 broth (Difco) supplemented with 0.5% glycerol, 10% albumin-dextrose complex, and 0.25% Tween 80 at 33 and 37°C for 7 and 3 days, respectively.

Isolation of *A. castellanii* variants. *A. castellanii* was infected with *L. pneumophila* in a 75-cm^2 tissue culture flask by a standard invasion assay protocol as described previously (11). Each flask, containing a monolayer of approximately 10^7 amoebae, was infected with 10^9 *L. pneumophila* amoebae for 30 min at 37°C in high-salt (HS) buffer (43). The monolayer was then washed once with HS buffer, 5 ml of HS buffer containing 100 μg of gentamicin per ml was added, and the mixture was incubated 2 h at 37°C, washed once with HS buffer, and incubated for 4 days at 37°C in 25 ml of HS buffer. The flasks were then washed four times with HS buffer and incubated at 24°C in the dark in 25 ml of PYG broth plus 200 μg of streptomycin per ml, 50 μg of kanamycin per ml, 2 μg of polymyxin B per ml, 100 μg of ampicillin per ml, 25 μg of tetracycline per ml, and 25 μg of chloramphenicol per ml for ~20 to 30 days. During this period, the monolayers were washed with HS buffer and fresh PYG broth plus antibiotic was added every 5 to 7 days. After this incubation, clones were isolated by limiting dilution (31). The first four rounds of selection were carried out with a single flask, whereas subsequent rounds of selection were done by splitting the output from round 4 into a total of 10 different flasks that were enriched for *L. pneumophila*-resistant variants independently. A total of 12 successive rounds of selection (4 as a single pool plus 8 independent rounds) were carried out in this manner, and clones were isolated from each round by limiting dilution and characterized for resistance to *L. pneumophila* infection. Each of the individual clones further characterized in this study was cloned by limiting dilution from a different flask after the final round of selection. The stability of each clone was tested by continuous passage in PYG broth for 6 months, followed by reevaluation of the frequencies of *Legionella* phagocytosis.

Phagocytosis assays. Phagocytosis assays were carried out in 24-well tissue culture dishes (Falcon) (10, 14). *A. castellanii* was seeded into the dishes at 1.5 × 10^5/well, allowed to adhere overnight at 23°C, washed once with HS buffer, and incubated in 1 ml of HS buffer for 1 h at 37°C, and 3 × 10^6 bacteria were added. After coincubation with the bacteria for 30 min, the amoebae were washed twice with HS buffer and incubated in HS buffer plus 100 μg of gentamicin per ml (legionellae) or 200 μg of amikacin per ml (mycobacteria) for 2 h at 37°C. The amoeba were then lysed by incubation for 10 min in 1 ml of sterile water, followed by vigorous pipetting. Dilutions were then plated on the appropriate medium to determine CFU counts.

We also used fluorescein isothiocyanate-conjugated latex beads (Molecular Probes, Eugene, Oreg.) and bacteria labeled with Oregon Green 418 (Molecular Probes) as described previously (13) to evaluate the phagocytic phenotype of the amoebal variants and macrophages treated with cellular inhibitors. In these assays, the cells were seeded in eight-well Permanox chamber slides (Nunc) at a density of 10^4/well and latex beads (1 μm; Molecular Probes) or fluorescent bacteria were added at a ratio of 20 per cell. After 30 min of coincubation, unbound beads or bacteria were removed by extensive washing with HS buffer. The cells were fixed in 4% paraformaldehyde in PBS buffer and mounted in 50% glycerol. The slides were examined under a Nikon TE300 fluorescence microscope with a fluorescein isothiocyanate filter. The percentage of cells that contained latex beads or bacteria and the number of beads or bacteria per cell were then determined by visual counts of 150 cells in random fields for each sample.

Assays for amoebal growth and killing by *L. pneumophila*. The ability of the *A. castellanii* variants to be killed by *L. pneumophila* was evaluated by measuring the viability of the amoebae after infection with the bacteria over time. The amoebae were infected with *L. pneumophila* in the same manner as described for phagocytosis assays. After gentamicin treatment, the amoebae were washed with HS buffer and incubated in HS buffer for 12 h prior to the initial determination of amoebal viability. Viability of amoebae was determined as described previously (12) at various time points. Basically, the amoebae were brought into suspension by pipetting, aliquots were stained with eosin Y (Sigma), and viable amoebae were counted with a hemacytometer (Hausser Scientific). Amoebal growth rates were determined in a similar manner but with incubation in standard PYG growth medium for 10 days and no bacterial infection.

Bactericidal activity of amoebal variants. Intracellular survival assays were carried out as described previously (12). *L. pneumophila* was added to a monolayer of 1.5 × 10^5 amoebae in 24-well tissue culture dishes at a multiplicity of infection (MOI) of 20 and incubated at 37°C for 30 min; the cells were washed three times with HS buffer and lysed at various time points with water. Survival is expressed as the percentage of CFU present at each time point compared to the number present at time zero (30 min), i.e., % survival = (CFU at T_x/CFU at T_0) × 100.

Amoebal morphology and lysosomal fusion frequencies. Light microscopy was carried out with live amoebae seeded at 37°C into a temperature-controlled closed perfusion chamber (Brook Industries) on a Nikon TE300 inverted microscope with differential-interference-contrast (DIC) optics.

Lysosomes were stained, and the frequency of fusion with the bacterial phagosome was determined by transmission electron microscopy essentially as described previously (12). After the amoebae were prelabeled with thorium dioxide (Polysciences), they were infected with *L. pneumophila* for 30 min. These samples and parallel unlabeled, uninfected amoeba samples for morphology studies were then fixed and prepared for electron microscopy as described previously (6, 12, 49).

Proteomic analysis. Amoebae were grown to log phase, and 2 × 10^7 cells were collected by centrifugation at 100 × *g* for 10 min. The pellets were washed twice with cold phosphate-buffered saline (PBS) and resuspended in 500 μl of lysis buffer (10 mM HEPES, 200 mM NaCl, 2 mM CaCl$_2$, 2.5 mM MgCl$_2$, 1% Triton X-100, 1 mM phenylmethylsulfonyl fluoride, 1× protease inhibitor cocktail). The suspension was incubated on ice for 30 min and sonicated for 10 s. The lysate was centrifuged at 5,000 × *g* at 4°C for 20 min to remove debris, and the supernatant was taken as the total protein sample. The concentration of protein was determined with the Bio-Rad protein assay (Bio-Rad Laboratories, Hercules, Calif.). Six hundred micrograms of protein from both wild-type and variant amoebae was then subjected to two-dimensional gel electrophoresis. The first isoelectric focusing (IEF) dimension was performed with immobilized pH gradient gel strips (17 cm, pH 3 to 10, nonlinear; Bio-Rad) and a Bio-Rad IEF cell. The strips were rehydrated with the protein samples in rehydration buffer {7 M urea, 2 M thiourea, 100 mM dithiothreitol (DTT), 4% (wt/vol) 3-[(3-cholamidopropyl)-dimethylammonio]-1-propanesulfonate (CHAPS), 0.001% bromophenol blue, 0.2% Bio-Lytes} at 50 V for 12 h in the IEF cell and focused at 10,000 V for a total of 80,000 V · h. Before being loaded on the second dimension, focused immobilized pH gradient strips were equilibrated in buffer I, which contained 6 M urea, 2% sodium dodecyl sulfate, 0.375 M Tris-HCl (pH 8.8), 20% glycerol, and 130 mM DTT, for 15 min and then in equilibration buffer II, in which DTT was replaced with 135 mM iodoacetamide, for another 15 min. The second-dimension electrophoresis was performed with a Bio-Rad Protein II xi apparatus on 10% acrylamide gels. After electrophoresis, the proteins were stained with Coomassie G-250 (Sigma, St. Louis, Mo.). Gel images were captured with a ProImage Analyzer camera and analyzed with Image Analyzer HD software (Genomic Solutions). To identify differences, all spots were compared to at least five reference spots that were consistently similar and well separated in all gels and quadruplicate pairs of independently prepared samples were used for each variant and wild-type amoebae.

MALDI-TOF mass spectrometry. For matrix-assisted laser desorption ionization–time of flight (MALDI-TOF) mass spectrometry, protein spots of interest were excised from the gel, washed, and analyzed as described previously (28). In brief, gel pieces were washed in 25 mM ammonium bicarbonate (NH$_4$HCO$_3$), pH 8.0, for 30 min, in 50% acetonitrile–25 mM NH$_4$HCO$_3$ for another 30 min, and finally with ultrapure water before complete dehydration in a vacuum centrifuge. The gel pieces were rehydrated with a minimum amount of sequence grade modified porcine trypsin solution containing 0.25 to 0.5 μg of protease, depending on the amount of protein. Digestion was performed at 37°C for 3 to 5 h. Mass spectra of the tryptic digests were acquired on a MALDI-TOF mass spectrometer operating in the reflector mode. A 0.5-ml volume of each digest solution (in 25 mM NH$_4$CO$_3$–10% acetonitrile) was deposited directly onto the sample probe on a dry thin layer of matrix made of α-cyano-4-hydroxy-*trans*-cinnamic acid mixed with nitrocellulose (4:3 [vol/vol] mixture of a saturated solution of α-cyano-4-hydroxy-*trans*-cinnamic acid in acetone and a solution consisting of 5 mg of nitrocellulose dissolved in 1 ml of isopropanol-acetone [1:1, vol/vol]). Deposits were washed with 5 ml of 0.1% trifluoroacetic acid before analysis. The peptide mass fingerprint obtained from each protein digested was analyzed with Mascot software (Matrix Science, London, United Kingdom) for protein identification.

Immunoprecipitation and Western analysis. The same number of cells from wild-type amoeba and the variants were collected and washed once with cold PBS, and cell lysates were prepared as described above. The cell lysates were immunoprecipitated with 10 μg of monoclonal antibody against hsp90 (StressGen Biotechnologies, Victoria, Canada) or α-tubulin (Sigma) while shaking at 4°C overnight. The immunocomplex was then incubated with protein G-Sepharose (Amersham) for 2 h, washed with lysis buffer four times, and fractionated by 10% sodium dodecyl sulfate-polyacrylamide gel electrophoresis. The proteins were then transferred to a nitrocellulose membrane (Poll) with a Bio-Rad transfer apparatus in accordance with the manufacturer's protocols. After incubation with 5% nonfat milk in TTBS (0.05% Tween 20, 20 mM Tris-HCl, pH 7.4) for 60 min, the membrane was washed once with TTBS and incubated with mouse

monoclonal antibodies (1:1,000) directed against hsp90 or α-tubulin at room temperature for 1 h. Membranes were washed three times for 10 min and incubated with a 1:3,000 dilution of horseradish peroxidase-conjugated anti-mouse immunoglobulin G (Sigma) for 1 h and detected with the ECL system (Amersham Pharmacia, Piscataway, N.J.). Densitometric analysis was carried out with ImageQuant software (Molecular Dynamics).

Pharmacological inhibitors of hsp90. The hsp90 inhibitors used in this study, geldanamycin (GA), radicicol (RD), herbimycin A (HB), and novobiocin (NB), were purchased from Sigma. After pretreatment of MH-S murine alveolar macrophages with each of the inhibitors at various concentrations, phagocytosis assays were performed in the same manner as described for amoebae, except that the cells were maintained in RPMI medium and washed with PBS. Intracellular survival assays were carried out with MH-S cells that had been either pretreated with the inhibitors and removed before addition of the bacteria or left in the medium throughout the entire experiment (24 h). For these assays, the cells were infected with bacteria in the same manner as for assays of survival in amoebae. The viability of the cells after treatment with these inhibitors and their solvents was determined with eosin Y and counting in a hemacytometer as described previously (12).

Quantitation of mitochondria in macrophages. The effects of hsp90 inhibitors on the number of mitochondria in MH-S murine alveolar macrophages was determined with a fluorescence-activated cell sorter. MH-S cells were treated with each inhibitor for 48 h, the cells were incubated with MitoTracker (Molecular Probes) at 20 mM for 30 min, excess dye was washed away, and at least 10,000 cells were analyzed for each sample on a Becton Dickinson FACScan flow cytometer.

Statistical analyses. Data presented are the means and standard deviations of triplicate samples from a representative experiment. All experiments were repeated at least three times, unless otherwise noted. Significance was determined by analysis of variance. P values of <0.05 were considered significant.

RESULTS

Isolation of stable *A. castellanii* variants. In order to better understand the host side of bacterium-host cell interactions, we took advantage of the single-celled nature of the environmental amoeba *A. castellanii*. When *A. castellanii* is infected with *L. pneumophila* at an MOI of 100 for 4 days, the entire monolayer of $>10^7$ amoebae is completely destroyed (11). Considering this information, it might be possible to use the amoebicidal activity of *L. pneumophila* as a direct selection for amoebae that have acquired changes in host cell components that play a role during interactions with bacteria. To test this hypothesis, we infected amoebae under conditions in which they would be almost entirely killed by *L. pneumophila* and grew those amoebae that survived this treatment. We carried out multiple infections in this manner for up to 12 rounds of selection. Individual amoebae were cloned from each round of selection by limiting dilution. Clones from the first through the fourth rounds were evaluated by comparing their frequencies of phagocytosis of *L. pneumophila* to that of wild-type amoebae. No significant differences were observed between the wild type and clones from these early rounds of selection (data not shown). However, four clones from the 12th round of selection, designated Ac3R, Ac4R, Ac6R, and Ac9R, were identified that displayed a decreased level of bacterial phagocytosis ($P < 0.025$; Fig. 1A). Although these data are for a ratio of bacteria per amoeba (MOI) of 20, we tested multiple MOIs ranging from 20 to 1 and all MOIs displayed the same level of decreased phagocytosis (data not shown). We examined the stability of the variants by continuous passage in the laboratory for more than 6 months, followed by reexamination of the phagocytic phenotype (Fig. 1A). These variants displayed a stable phagocytic phenotype after continuous laboratory passage. In addition, none of the variants grew at a rate different
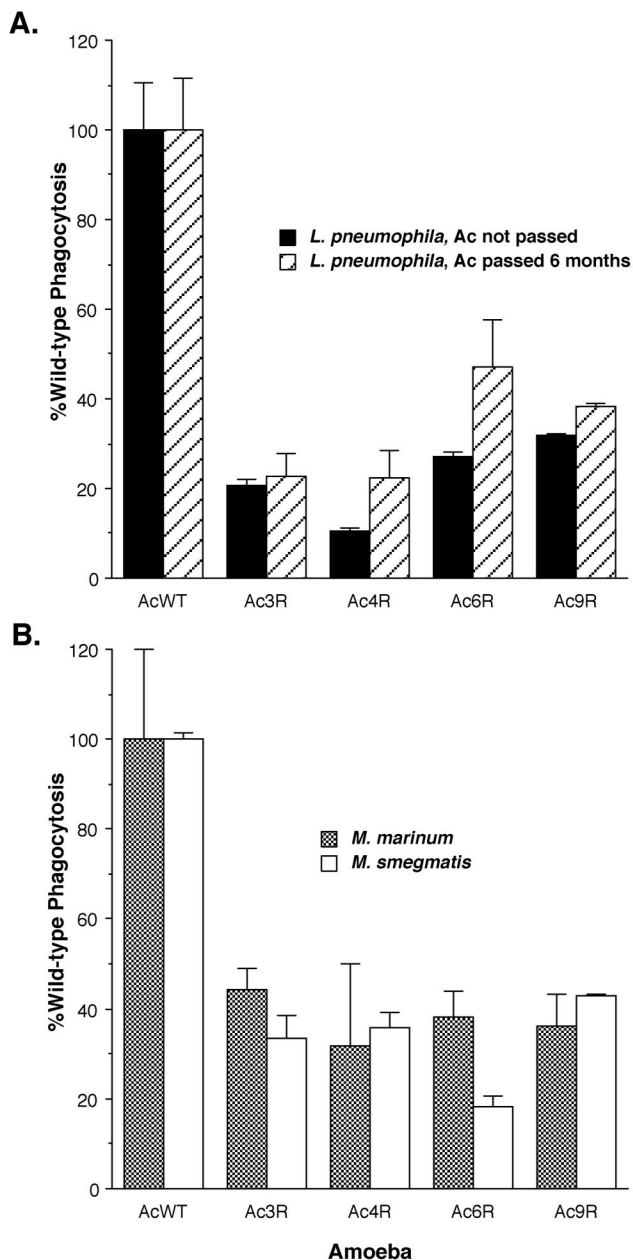

FIG. 1. Phagocytosis of *L. pneumophila* (A) or *M. smegmatis* and *M. marinum* (B) by *A. castellanii* (Ac) variants calculated as the percentage of that displayed by wild-type amoebae (AcWT) under the same conditions. Phagocytosis assays were carried out by coincubating the bacteria with cells for 30 min and evaluating the number of bacterial CFU that are intracellular at the end of this time period. Amoebal variants (Ac3R, Ac4R, Ac6R, and Ac9R) were characterized for *L. pneumophila* phagocytosis immediately after cloning by limiting dilution and after passage during continuous culture for 6 months. The data points and error bars represent the means and standard deviations, respectively, of assays done in triplicate. The data shown are representative of at least three independent experiments.

from that of wild-type amoebae ($P > 0.1$) in standard PYG laboratory medium (data not shown).

Amoebal variants are defective in phagocytosis of mycobacteria. We examined the specificity of the phagocytic defect with
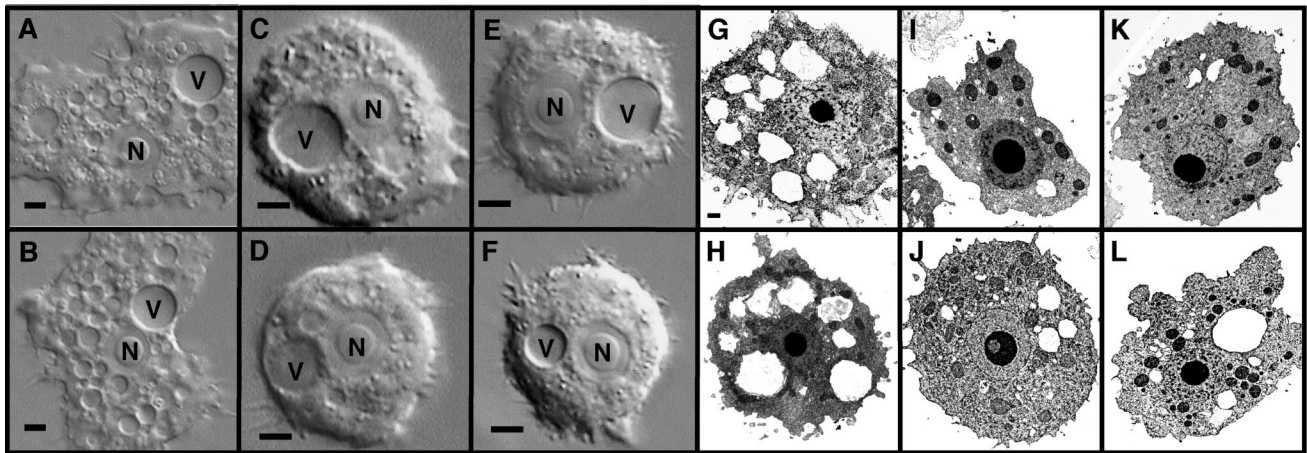
FIG. 2. Morphology of wild-type *A. castellanii* (A, B, G, H) and amoebal variants Ac3R (C, I), Ac4R (E, K), Ac6R (D, J), and Ac9R (F, L) by DIC microscopy (A to F) and transmission electron microscopy (G to L). The *A. castellanii* nucleus (N) and contractile vacuole (V) are visible in each DIC panel. The bar in each DIC panel is 10 μm. The bar in panel G is 1 μm and applies to panels G to L. Electron-dense particles in panels G to L are mostly mitochondria with a single nucleus and nucleolus visible. Electron-transparent regions are vacuolar compartments with the contractile vacuole commonly appearing as the largest vacuole.

mycobacteria as phagocytic particles. We chose both pathogenic and nonpathogenic mycobacterial species, *Mycobacterium marinum* and *Mycobacterium smegmatis*, respectively, for these studies. The amoebal variants were defective for phagocytosis of both *M. smegmatis* and *M. marinum* at levels similar to that observed for *L. pneumophila* (Fig. 1B). These observations suggest that the defect present in these amoebae is relatively broad and likely to affect a number of bacterial species, since mycobacteria (gram positive) and legionellae (gram negative) are very distantly related.

Amoebal variants are morphologically different from the wild type. To further characterize these amoebal variants, we examined their morphology by light and electron microscopy. Light microscopy demonstrated that the variants contain fewer intracellular vacuoles and have a more rounded shape than wild-type amoebae (Fig. 2). Electron microscopy confirmed the relative paucity of intracellular vacuoles in the variants and

suggested that the number of mitochondria is greater in the variants than in the wild type (Fig. 2). We quantitated the number of vacuoles and mitochondria in both the variants and the wild type. The number of intracellular vacuoles is significantly lower in all variants than in the wild type, and the number of mitochondria is significantly higher in Ac3R and Ac9R (Table 1). The morphological differences observed are stable over 6 months of passage in the laboratory. These observations suggest that the amoebal variants carry differences that affect more than one cellular characteristic and, as a result, might affect all phagocytic events.

Amoebal variants are not defective for phagocytosis of latex beads. To test whether the phagocytic defect is due to a general cellular defect, rather than specific to bacterial uptake, we examined the ability of these amoebae to take up latex beads. Although all of the amoebal variants displayed reduced uptake of fluorescent bacteria by microscopy, both the number of beads per cell and the percentage of cells that phagocytosed at least one bead were the same for all mutants as for wild-type amoebae (Table 2). Although the mean values for variant Ac9R appear somewhat lower than for the wild type, this difference is not significant ($P > 0.2$). These observations sug-

TABLE 1. Structural characteristics of the amoebae used in this study

Amoebae	No. of vacuoles/cell[a]	No. of mitochondria/cell
Wild type	7.8 ± 2.5	9.2 ± 2.7
Ac3R	4.5 ± 1.9[b]	12 ± 4.3[b]
Ac4R	4.4 ± 2.2[b]	11 ± 3.5
Ac6R	4.1 ± 2.2[b]	11 ± 5.3
Ac9R	4.5 ± 2.1[b]	15 ± 4.4[b]
6-mo wild type	6.1 ± 1.5	9.3 ± 2.6
6-mo Ac3R	4.2 ± 1.2[b]	14.4 ± 3.3[b]
6-mo Ac4R	4.8 ± 1.2[b]	11.4 ± 2.7
6-mo Ac6R	5.1 ± 1.5[b]	12.0 ± 3.1
6-mo Ac9R	4.8 ± 1.4[b]	14.8 ± 2.9[b]

[a] Number of food vacuoles (excluding contractile vacuole) per amoeba in two counts of 50 cells each from amoebal variants and the wild type immediately after isolation and following passage in the laboratory for 6 months. The results are the means ± standard deviations. The data are representative of at least two independent experiments.
[b] Significantly different ($P < 0.05$) from the result for wild-type *A. castellanii*.

TABLE 2. Phagocytosis of latex beads and bacteria by amoebae

Amoebae	% Phagocytosis[a]		No. of particles/amoeba	
	Beads	Bacteria	Beads	Bacteria
Wild type	90 ± 16	71 ± 5.3	3.4 ± 2.5	3.2 ± 0.1
Ac3R	92 ± 15	37 ± 3.1[b]	2.9 ± 2.1	2.0 ± 0.1[b]
Ac4R	91 ± 17	37 ± 9.4[b]	3.4 ± 2.4	3.0 ± 0.2
Ac6R	91 ± 19	53 ± 9.8[b]	3.4 ± 2.3	2.7 ± 0.2[b]
Ac9R	78 ± 19	55 ± 10[b]	2.2 ± 1.6	2.7 ± 0.2[b]

[a] Percentage of amoebae that contained at least one bacterium (*L. pneumophila*) or bead as determined by fluorescence microscopy. The results are the means ± standard deviations for three counts of 50 amoebae. The data are representative of at least two independent experiments.
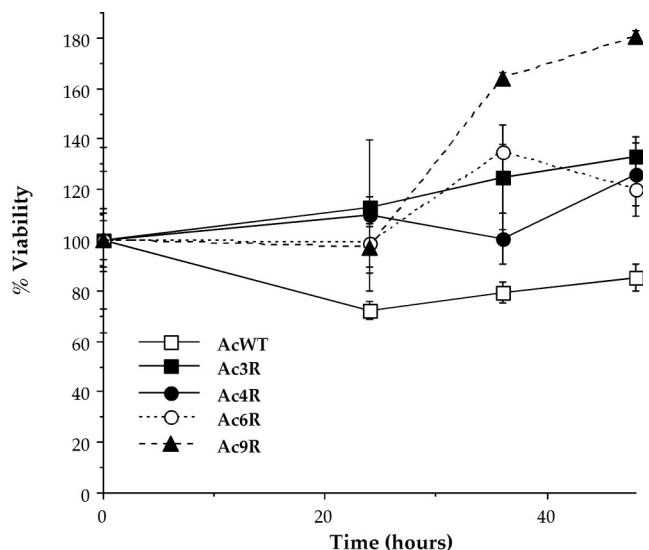[b] Significantly different ($P < 0.05$) from the result for wild-type *A. castellanii*.

FIG. 3. Percent viability of the *A. castellanii* wild type (AcWT) and variant clones Ac3R, Ac4R, Ac6R, and Ac9R after infection with *L. pneumophila*. For viability studies, the amoebae were first infected with bacteria in the same manner as for phagocytosis assays, followed by removal of extracellular bacteria and determination of amoebal viability at various time points. Time zero is 12 h after addition of bacteria. The viability of each amoeba was arbitrarily set to 100% at the first time point. Data points and error bars represent the means and standard deviations, respectively, of assays done in triplicate. The data shown are representative of at least three independent experiments.

gest that the phagocytic phenotype of these variants is at least somewhat specific to their interactions with bacteria, rather than affecting uptake of all phagocytic particles, and is not solely the result of rapid intracellular killing, since enumeration of fluorescent bacterial particles phagocytosed is not dependent on bacterial viability.

Amoebal variants are resistant to killing by *L. pneumophila*. We infected each of the amoebal variants with *L. pneumophila* for 30 min and compared their subsequent viability over time (Fig. 3). All of the amoebal variants were more resistant to killing by *L. pneumophila* than were wild-type amoebae ($P < 0.01$). Thus, these variants display an *L. pneumophila*-resistant phenotype, possibly resulting from decreased uptake of the bacteria or increased bactericidal activity.

Amoebal variants display enhanced bactericidal activity. We monitored the intracellular survival of *L. pneumophila* in wild-type amoebae and the variants over time. All amoebal variants displayed higher ($P < 0.01$) bactericidal activity than did wild-type amoebae (Fig. 4). Normally, by 10 h after infection at least some bacterial replication is observable in wild-type amoebae, but replication is not observed with each of the variants until later and the bacteria are killed at higher levels early during infection. In order to determine whether the lower levels of phagocytosis leading to fewer intracellular bacteria is the reason for the increased ability of the amoebae to kill them, we tested survival and replication at a lower MOI than 20 bacteria per amoeba, which is the standard condition, in wild-type amoebae (Fig. 4). On the basis of these data, there is no correlation between the numbers of bacteria phagocytosed and their ability to survive and replicate in wild-type amoebae.
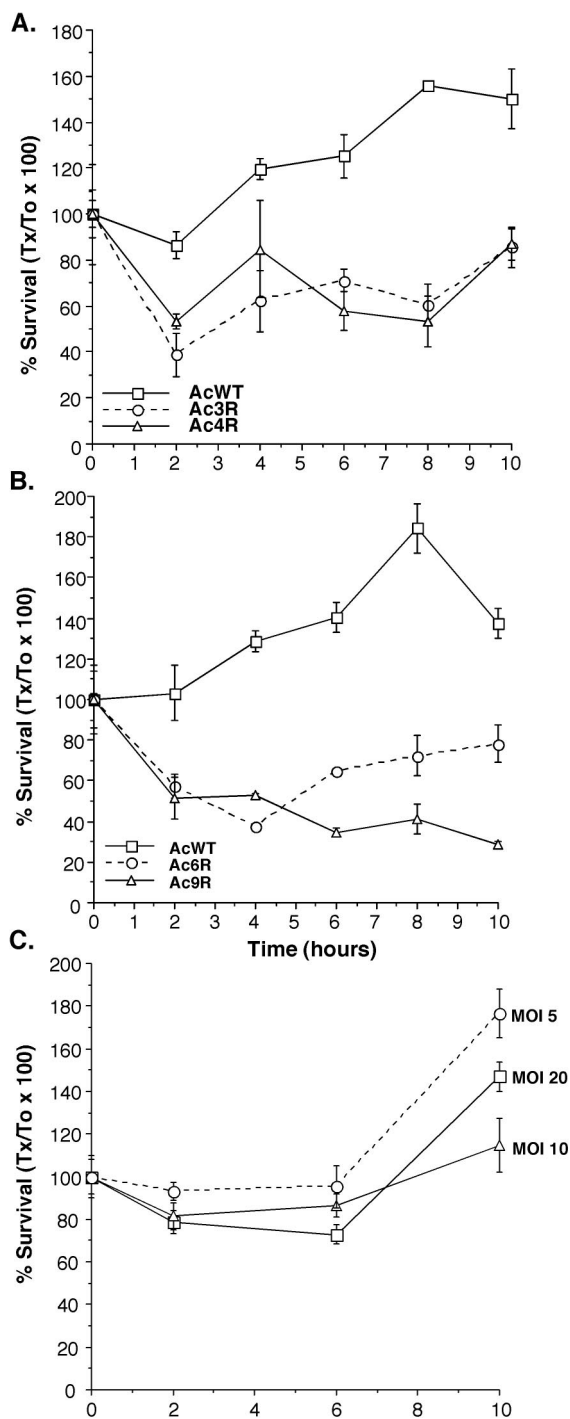

FIG. 4. Survival of *L. pneumophila* in wild-type (AcWT) *A. castellanii* and amoebal variants Ac3R and Ac4R (A) or Ac6R and Ac9R (B) and in wild-type amoebae when different MOIs were used on the basis of the ratio of the number of bacteria available for phagocytosis per amoeba (C). Amoebae were infected in the same manner as for phagocytosis assays, and the number of intracellular bacterial CFU was determined at various time points (T_x) relative to time zero (T_0, 30 min). Data points and error bars represent the means and standard deviations, respectively, of assays done in triplicate. The data shown are representative of at least three independent experiments.
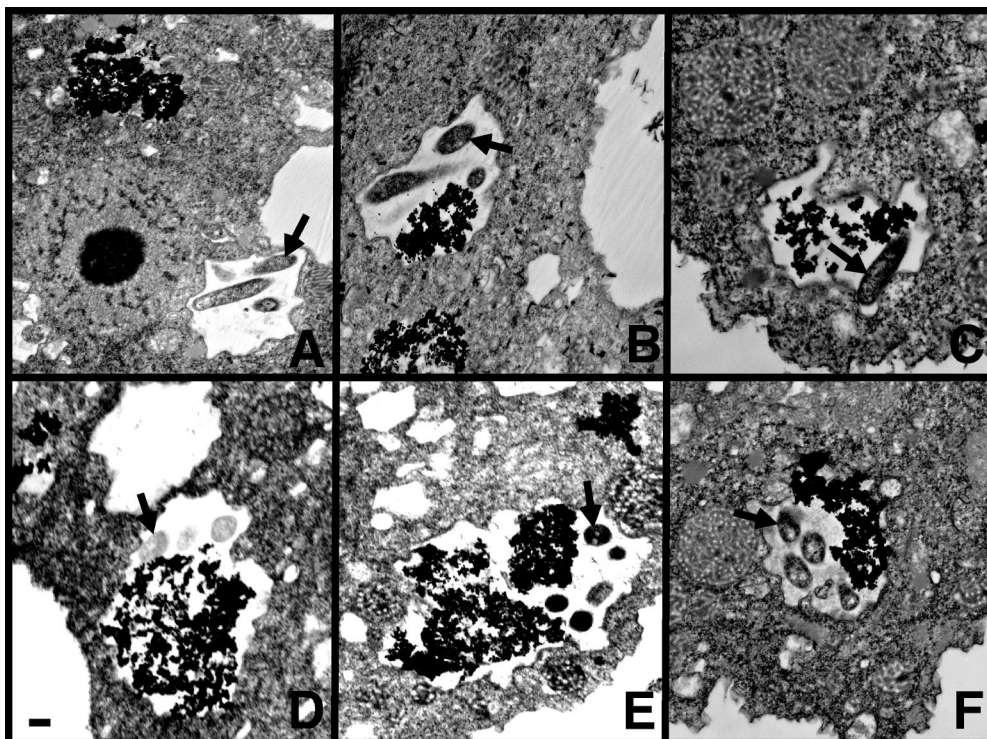
FIG. 5. Transmission electron micrographs of *L. pneumophila* vacuoles that have not fused (A) and that have fused (B to F) with lysosomes in thorium dioxide-labeled wild-type *A. castellanii* (A, D) and clones Ac3R (B), Ac4R (C), Ac6R (E), and Ac9R (F) at 30 min postinfection. Granular, electron-dense material is thorium dioxide that has accumulated in lysosomes. After the amoebae were prelabeled with thorium dioxide and the excess label was removed, the amoebae were infected with bacteria in the same manner as for phagocytosis assays prior to fixation at various time points and preparation for electron microscopy. When thorium dioxide is present in the same intracellular compartment with bacteria, they are considered to have fused with lysosomes. The bar in the bottom left of panel D is 1 μm and applies to all of the panels. Arrows indicate bacteria in each panel.

These observations suggest that there are differences in how the amoebal variants interact with bacteria at early time points during signal transduction, phagocytosis, and/or trafficking.

Amoebal variants circumvent inhibition of lysosomal fusion by *L. pneumophila*. Inhibition of lysosomal fusion by *L. pneumophila* is a key factor in their ability to survive and replicate in macrophages (33) and amoebae (7). Since we observed a decrease in the ability of *L. pneumophila* to survive in the amoebal variants, differences in trafficking of the bacterial phagosome may be at least partially responsible. We investigated this possibility by transmission electron microscopy with thorium dioxide as a marker for the lysosomal compartment (Fig. 5). The frequency of lysosomal fusion with the *L. pneumophila* vacuole in the variants was significantly higher ($P < 0.02$) than for wild-type *A. castellanii* (Table 3). These data suggest that one of the factors involved in the enhanced bactericidal activity of the amoebal variants is a decreased ability of *L. pneumophila* to inhibit phagosome-lysosome fusion in these cells.

Amoebal variants have a limited number of protein differences. Since the amoebal variants differ from the wild type in a number of phenotypic characteristics, we carried out proteomic analysis to identify any molecular differences from wild-type amoebae. Analysis of total proteins from the variants resulted in the identification of three to six proteins that are absent and three to four that are at lower levels in each of the

variants compared to wild-type amoebae. Although all of these differences were consistent over four sets of gels run in parallel, three proteins were consistently at lower levels or absent in all four of these variants (Fig. 6). These observations suggest that some or all of these three proteins are important for the phenotypic characteristics of the amoebal variants.

Hsp90 is down-regulated in all of the amoebal variants. Each of these spots was excised and subjected to MALDI-TOF mass spectrometry in order to determine the identity of the protein that it represents. Two of these spots matched, at very high significance, actin and hsp90, and the third spot displayed

TABLE 3. Fusion of *L. pneumophila* vacuoles with lysosomes

Amoebae	% Fusion[a]	
	30 min	120 min
Wild type	31 ± 5	46 ± 6
Ac3R	57 ± 2[b]	64 ± 4[b]
Ac4R	63 ± 7[b]	68 ± 6[b]
Ac6R	51 ± 2[b]	72 ± 3[b]
Ac9R	55 ± 1[b]	62 ± 5[b]

[a] Percentage of bacterial (*L. pneumophila*) vacuoles containing thorium. The results are the means ± standard deviations for three counts of 50 amoebae in different sections of the same preparation. The data are representative of at least two independent experiments.
[b] Significantly different ($P < 0.02$) from the result for wild-type *A. castellanii*.
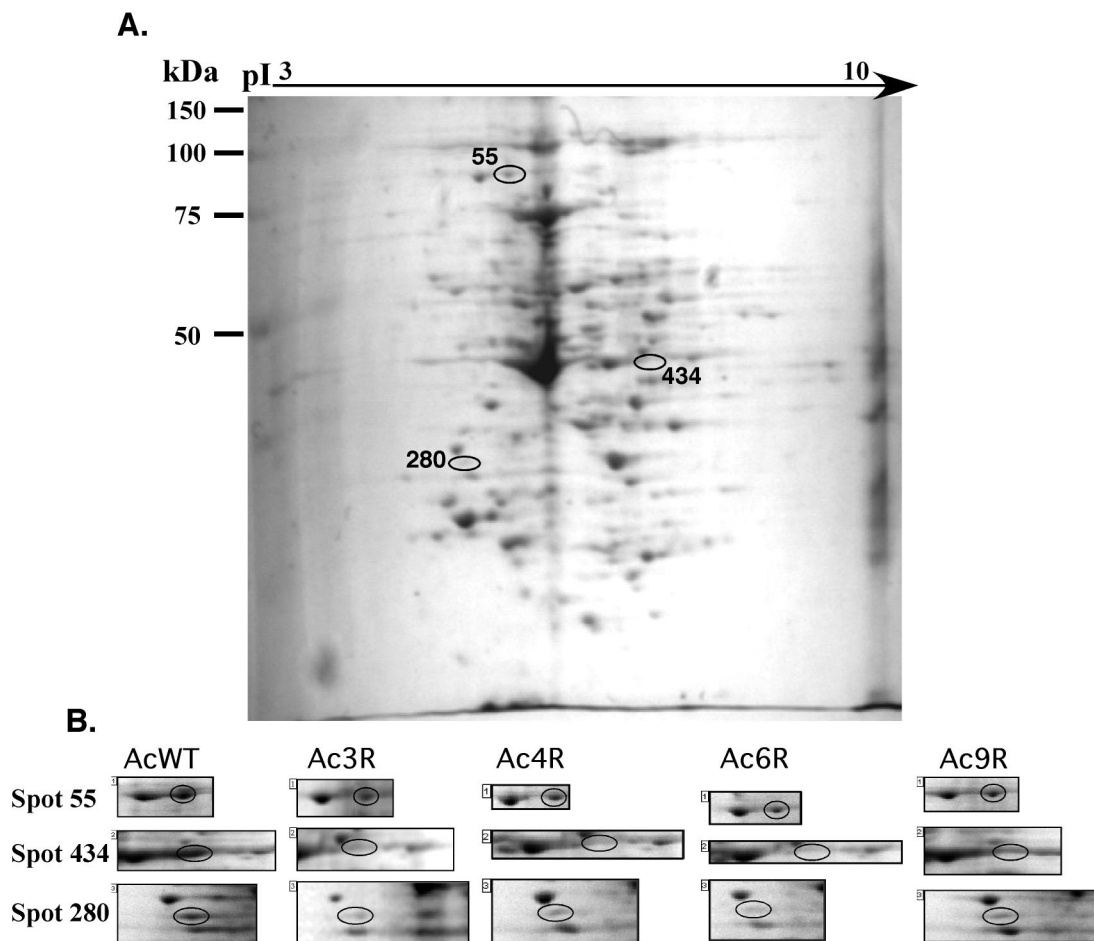
A.

B.

FIG. 6. Proteomic analysis of differences between wild-type (AcWT) and variant amoebae. Example of a single Coomassie-stained two-dimensional polyacrylamide gel electrophoresis gel of total proteins from amoebal variant Ac3R (A) and comparative analysis (B) of spots 55, 280, and 434, which were found in all variants at lower levels than in the wild type. During this analysis, all spots on each gel were compared to a minimum of five reference spots that were consistently present and clearly separated in all gels. Once differences were found, they were reexamined in a minimum of three independent experiments and quadruplicate pairs of gels to evaluate whether the differences were consistent.

some similarity to cyclophilin D but did not reach significance (Table 4). The presence of low levels of hsp90 in the amoebal variants was confirmed by Western analysis of proteins immunoprecipitated with an anti-hsp90 monoclonal antibody (Fig. 7). Identical volumes of the same amoebal lysate were also immunoprecipitated with α-tubulin monoclonal antibody as a control for protein loading differences. Densitometric analysis of the relative levels of hsp90 compared to α-tubulin demonstrated that all amoebal variants have between 5- and 20-fold lower levels of hsp90 than the wild type.

Inhibition of hsp90 in macrophages increases mitochondrial numbers and bacterial phagocytosis and survival. Since hsp90 is thought to interact with both actin (36, 48) and cyclophilins (68, 72), as well as a number of other cellular proteins (53), it is possible that this protein is a key factor in the phenotypic characteristics of the variants. A number of specific inhibitors exist for hsp90 in mammalian cells, allowing us to test whether this protein plays a role in phagocytosis of bacteria. However, since none of these inhibitors produced the expected effects in amoebae (data not shown), we conducted inhibitor studies with mammalian cells. These inhibitors pro-

duced similar results with both J774A.1 (data not shown) and MH-S murine macrophage cell lines. We found that all inhibitors of hsp90 significantly increased fluorescent staining with the mitochondrion-specific dye MitoTracker (Table 5). In addition, these inhibitors decreased phagocytosis of *L. pneumophila* in a dose-dependent manner whether viable intracellular bacteria or microscopy was used to determine the number of particles phagocytosed, yet the inhibitors did not reduce the phagocytosis of latex beads (Fig. 8A). Furthermore, intracellular survival and replication of *L. pneumophila* were reduced in macrophages pretreated with hsp90 inhibitors prior to infection (Fig. 8B). To ensure that the inhibitors did not directly inhibit the growth of the bacteria, we examined survival and replication of *L. pneumophila* when the inhibitors were present during bacterial interactions with macrophages. Most of the inhibitors, with the exception of NB, produced similarly reduced levels of *L. pneumophila* survival and replication either when they were used to pretreat the cells or when they were present throughout the experiment (Fig. 8B). When NB was present throughout the experiment, no bacterial replication was observed, suggesting that this inhibitor affects bacterial

TABLE 4. MALDI-TOF analysis of differentially expressed proteins

Spot no.	Gene	Molecular mass (kDa)		No. of peptides[a]	Score[b]	Sequence[c]
		Estimated	Actual			
55	gi:1708316 hsp90	85	80	8	242	ELISNASDALDK HFSVEGQLEFK GIVDSEDLPLNISR
280	gi:5739196 Cyclophilin D	20	19	3	15	QGNTPLGR IGCLSMANAGK
434	gi:71629 Actin	40	42	12	437	IIAPPER AGFAGDDAPR GYSFTTTAER DSYVGDEAQSKR IWHHTFYNELR EEYDESGPSIVHR SYELPDGQVITIGNER VAPEEHPVLLTEAPLNPK

[a] Number of peptides that matched by Mascot (www.matrixscience.com) on the spectra obtained from each protein spot.
[b] Scores of >23 are considered significant ($P < 0.05$).
[c] Amino acid sequences of unique peptide matches.

replication and pretreatment of the macrophages may have some degree of inhibitory effect on the bacteria themselves. None of these inhibitors or their solvents, at the concentrations and time points used, affected macrophage or bacterial viability (data not shown). These observations support a role for hsp90 in cellular pathways that are important for uptake and/or killing of bacteria in phagocytic cells.

FIG. 7. Levels of hsp90 or α-tubulin in wild-type (AcWT) and variant (Ac3R and Ac4R) amoebae as determined by Western analysis of identical volumes of the same amoebal lysate immunoprecipitated with anti-hsp90 or α-tubulin monoclonal antibody (A) and densitometric analysis of the levels of hsp90 calculated relative to the α-tubulin present in each amoebal lysate (B). The data shown are representative of at least three independent experiments.

DISCUSSION

Our selection strategy has allowed the isolation of four *A. castellanii* variants that display lower levels of bacterial phagocytosis than wild-type amoebae. Potential mechanisms that might lead to this phenotype include loss or alteration of a receptor, modification of signaling pathways, cytoskeletal changes affecting phagocytosis, and increased bactericidal activity. Each of these clones displays differences in multiple stages during its interactions with bacteria. However, through the use of two-dimensional polyacrylamide gel electrophoresis we were able to evaluate differences in the protein profiles of these clones and identify those that differ from wild-type amoebae. On the basis of our data, hsp90 appears to be important for the observed phenotypic traits of these variants. hsp90 is very conserved across species and is an essential stress protein in eukaryotic cells (38, 74). Since hsp90 has truly pleiotropic activities (53), it is possible that lower levels of this single protein are responsible for all of the differences between these variants and wild-type amoebae.

Although these are the first *A. castellanii* variants identified that affect interactions with *L. pneumophila*, another model
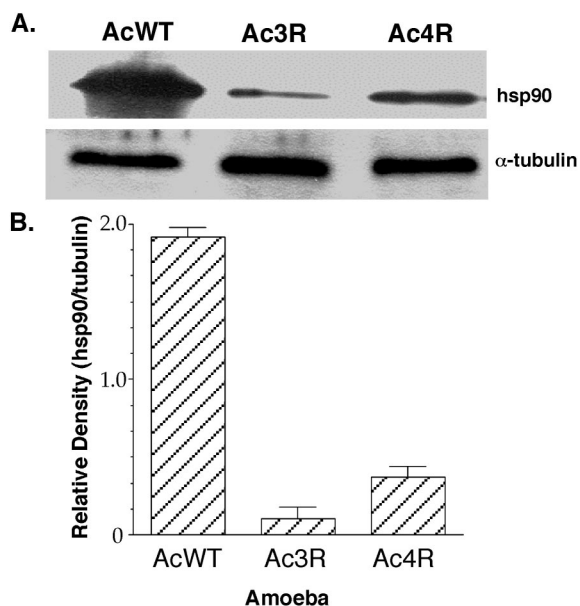
TABLE 5. Mitochondria in macrophages treated with hsp90 inhibitors

Treatment	Mitochondrial fluorescence[a]
Medium	67.7 ± 0.7
500 nM RD	80.4 ± 1.6[b]
500 nM GA	101.2 ± 3.8[b]
1 mM NB	83.0 ± 2.5[b]
1 μM HB	114.1 ± 0.0[b]

[a] Mean fluorescence ± standard deviation of 10,000 cells as measured by flow cytometry after staining of hsp90 inhibitor-treated MH-S murine alveolar macrophages with the mitochondrion-specific fluorescent marker MitoTracker. The data are representative of at least two independent experiments. The inhibitors used were RD, GA, NB and HB.
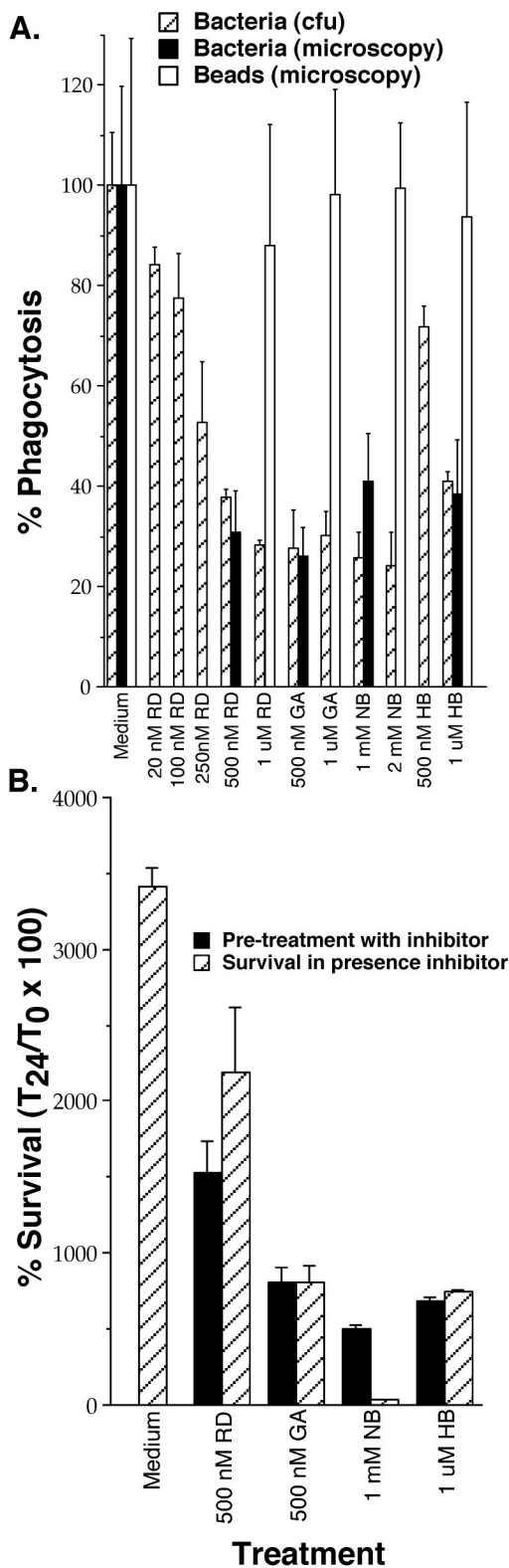[b] Significantly different ($P < 0.01$) from the result for medium.

system for *L. pneumophila* host-pathogen interactions has been used for analysis of host factors involved, i.e., *Dictyostelium discoideum* (30, 64). Interestingly, most of the *D. discoideum* mutants examined that were considered good candidates for playing a role in host-pathogen interactions increased rather than decreased the susceptibility of *D. discoideum*. Only a G_B mutant, which is defective for all types of trimeric G-protein signaling, displayed a slightly reduced ability to support growth of *L. pneumophila* (64). Thus, the current strategy of enriching for bacterium-resistant variants has allowed the identification of a second host factor involved in host cell-*L. pneumophila* interactions without the cumbersome task of screening a large number of mutants with changes in candidate genes of interest. Possibly, the enrichment method developed in the present study could be applied to *D. discoideum* or pools of *D. discoideum* mutants. Certainly, this procedure could be improved by conducting mutagenesis of the amoebae, to increase the frequency at which variants would be found, and enriching for variants from a number of independent pools, to prevent the isolation of siblings, which was most likely responsible for our observation that all variants displayed decreased levels of hsp90. One limitation of this approach with *D. discoideum* is that *L. pneumophila* does not infect and kill *D. discoideum* (30, 64) as efficiently as it does *A. castellanii*. Furthermore, although *D. discoideum* has many similarities to other environmental protozoa, there is no evidence that it can serve as a natural host for *L. pneumophila*, possibly because *D. discoideum* prefers soil habitats (5) and *L. pneumophila* prefers aquatic environments (24, 25). Thus, the fact that *A. castellanii* is a natural host for *L. pneumophila* may prove to be a valuable asset for further analysis of host-pathogen interactions.

The *A. castellanii* variants we have isolated display decreased vacuolation, and two of them have an increased number of mitochondria. Previous observations of macrophages suggest that an increased number of mitochondria correlate with activation of macrophages (15, 16) and greater resistance to infection (35). In macrophages, resistance to infection may result from an enhanced ability to carry out oxidative phosphorylation during a respiratory burst (50). A respiratory burst results in secretion of extracellular ATP (61, 70), which is known to increase the production of reactive oxygen and nitrogen species (44, 61, 70). Interestingly, a role for hsp90 in control of superoxide production in host cells has recently been suggested (65). Further characterization of these variants may provide

FIG. 8. Phagocytosis of *L. pneumophila* (Bacteria) or 1-μm latex beads (Beads) by MH-S murine alveolar macrophages (A) and survival and replication of *L. pneumophila* over 24 h within these same cells (B). Assays were carried out in the presence and absence (Medium) of various concentrations of specific hsp90 inhibitors. Phagocytosis assays for bacteria [Bacteria (cfu)] were carried out in the same manner as described for amoebae and by evaluating the number of bacterial CFU that were intracellular at the end of this time period. Phagocytosis of bacteria [Bacteria (microscopy)] and beads [Beads (microscopy)] was quantitated by fluorescence microscopy to determine the percentage of cells that contained at least one particle for three counts of 50 amoebae. Survival and replication assays were carried out by first pretreating the cells with the inhibitor and either removing it by washing prior to infection (Pretreatment with inhibitor) or pretreatment followed by infection and maintenance of the presence of the inhibitor throughout the remainder of the experiment (Survival in presence inhibitor). Survival and replication were evaluated at 24 h postinfection (T_{24}) relative to time zero (T_0, 30 min). The inhibitors used were RD, GA, NB, and HB. Phagocytosis was calculated as the percentage of that displayed in the absence of any inhibitor. Data points and error bars represent the means and standard deviations, respectively, of assays done in triplicate. The data shown are representative of at least three independent experiments.

insight into the role of hsp90 in bactericidal mechanisms, similar to those found in mammalian macrophages.

Signaling events that affect intracellular trafficking and bactericidal activity may be triggered by bacteria binding to different host cell receptors. hsp90 is known to interact with a number of different cell surface receptors, including scavenger receptors (45) and steroid receptors (21). It has also been suggested that hsp90 itself can serve as a receptor for either lipopolysaccharide (71) or specific bacterial proteins (34). In addition, hsp90 plays an important role in a number of receptor-mediated signal transduction pathways (53, 57). This concept fits well with the observation that phagocytosis of latex beads is triggered by mechanical contact rather than a receptor-mediated pathway (73). Effects on receptors or signal transduction may be responsible for the bactericidal phenotype, but it is possible that trafficking of the bacterial vacuole is affected directly considering that hsp90 can play an important role in receptor trafficking (18, 27). Further analysis of these variants should allow us to differentiate between these possibilities.

Although all of the variants display lower levels of hsp90, they show slightly different phenotypic characteristics and have lower levels of other proteins as well. There are two simple explanations for the differences in phenotype and differences in protein profile. First, the levels of hsp90 vary from two- to fivefold less in the amoebal variants. Since hsp90 can affect the turnover of proteins that it interacts with (17, 26, 46, 60), it is conceivable that the levels of other hsp90-associated proteins would be affected differently depending on the levels of hsp90 present. This possibility is supported by the fact that both actin (36, 48) and cyclophilins (68, 72) have been previously shown to interact with hsp90. Possibly, hsp90 is involved in modification of actin, since only actin migrating at a specific pI is at lower levels in the variants than in the wild type and at least three forms of actin are normally present in eukaryotic cells (56, 67). Second, since multiple rounds of selection were carried out, it is possible that secondary mutations were acquired that are involved in some of the more subtle differences between the variants. Characterization of the other protein differences and either reconstruction of the variants through molecular means or complementation analyses should help to differentiate between these possibilities.

Although known inhibitors of hsp90 in mammalian cells had no effect in amoebae, it is likely that this result is due to differences between the amoebal and mammalian proteins, transport of the inhibitors, or other aspects of amoebal physiology. GA and the closely related compound HB are actinomycete fermentation products of the benzoquinone ansamycin class (62). Ansamycin antibiotics such as GA and HB bind at the ATP-binding site in the N-terminal domain of hsp90 and disrupt the ATPase activity of hsp90, which is essential for its chaperone activity in vivo (29, 51, 54, 58). Although RD has no significant structural similarity to GA or HB, it also binds to the N-terminal nucleotide-binding domain of hsp90 and inhibits the inherent ATPase activity of hsp90 (58). However, RD shows a greater affinity for the nucleotide binding site than does GA. Unlike GA, RD causes no significant conformational changes (58). The binding site for NB lies within the C-terminal region of hsp90 (40, 41). The second C-terminal ATP-binding site is responsible for autophosphorylation of hsp90

(37). GA does not interfere with autophosphorylation of hsp90 and hence does not bind to the C-terminal ATP-binding site (37). Since all of these inhibitors differ with respect to the mechanism of hsp90 inhibition and specific chemical structure, it is unlikely that nonspecific effects are responsible for the observed phenotypic changes in macrophages. It is compelling that hsp90 inhibitors produce a phagocytic defect in macrophages similar to that observed in amoebae. Furthermore, hsp90 inhibitors also reduce bacterial survival and replication in macrophages, as well as increase the numbers of mitochondria. On the basis of these data, it is unlikely that the other protein differences observed play as important a role in the phenotypic characteristics of the amoebal variants as hsp90.

Overall, these studies demonstrate, for the first time, a role for hsp90 in the interactions of phagocytic cells with bacteria. This protein may influence the mechanisms of phagocytosis, bactericidal activity, or a combination of these cellular processes. Since there are direct links between the mechanism of phagocytosis and subsequent intracellular events, it may be difficult to differentiate between these possibilities. However, careful examination of phagocytic and signal transduction pathways in the variants and the wild type should provide insight into the role of hsp90. Thus, the observation that hsp90 plays a role in early bacterium-phagocyte interactions is likely to assist in elucidation of the cellular pathways involved.

REFERENCES

1. Abd, H., T. Johansson, I. Golovliov, G. Sandstrom, and M. Forsman. 2003. Survival and growth of *Francisella tularensis* in *Acanthamoeba castellanii*. Appl. Environ. Microbiol. **69:**600–606.
2. Allen, P. G., and Dawidowicz. 1990. Phagocytosis in *Acanthamoeba*. I. A mannose receptor is responsible for the binding and phagocytosis of yeast. J. Cell. Physiol. **145:**508–513.
3. Allen, P. G., and E. A. Dawidowicz. 1990. Phagocytosis in Acanthamoeba. II. Soluble and insoluble mannose-rich ligands stimulate phosphoinositide metabolism. J. Cell. Physiol. **145:**514–521.
4. Barker, J., and M. R. W. Brown. 1994. Trojan horses of the microbial world: protozoa and the survival of bacterial pathogens in the environment. Microbiology **140:**1253–1259.
5. Bonner, J. T. 1944. A descriptive study of the development of the slime mold *Dictyostelium discoideum*. Am. J. Bot. **31:**175–182.
6. Bowers, B., and E. D. Korn. 1968. The fine structure of *Acanthamoeba castellanii*. I. The trophozoite. J. Cell Biol. **39:**95–111.
7. Bozue, J. A., and W. Johnson. 1996. Interaction of *Legionella pneumophila* with *Acanthamoeba castellanii*: uptake by coiling phagocytosis and inhibition of phagosome-lysosome fusion. Infect. Immun. **64:**668–673.
8. Brown, R. C., H. Bass, and J. P. Coombs. 1975. Carbohydrate binding proteins involved in phagocytosis by *Acanthamoeba*. Nature **254:**434–435.
9. Cirillo, J. D. 1999. Exploring a novel perspective on pathogenic relationships. Trends Microbiol. **7:**96–98.
10. Cirillo, J. D., S. L. G. Cirillo, L. Yan, L. E. Bermudez, S. Falkow, and L. S. Tompkins. 1999. Intracellular growth in *Acanthamoeba castellanii* affects monocyte entry mechanisms and enhances virulence of *Legionella pneumophila*. Infect. Immun. **67:**4427–4434.
11. Cirillo, J. D., S. Falkow, and L. S. Tompkins. 1994. Growth of *Legionella pneumophila* in *Acanthamoeba castellanii* enhances invasion. Infect. Immun. **62:**3254–3261.
12. Cirillo, J. D., S. Falkow, L. S. Tompkins, and L. E. Bermudez. 1997. Interaction of *Mycobacterium avium* with environmental amoebae enhances virulence. Infect. Immun. **65:**3759–3767.
13. Cirillo, S. L., L. Yan, M. Littman, M. M. Samrakandi, and J. D. Cirillo. 2002. Role of the *Legionella pneumophila rtxA* gene in amoebae. Microbiology **148:**1667–1677.
14. Cirillo, S. L. G., L. E. Bermudez, S. H. El-Etr, G. E. Duhamel, and J. D.

Cirillo. 2001. *Legionella pneumophila* entry gene *rtxA* is involved in virulence. Infect. Immun. **69:**508–517.

15. **Cohn, Z. A., and B. Benson.** 1964. The differentiation of mononuclear phagocytes: morphology, cytochemistry and biochemistry. J. Exp. Med. **121:**153–169.

16. **Cohn, Z. A., J. G. Hirsch, and M. E. Fedorko.** 1965. The in vitro differentiation of mononuclear phagocytes. IV. The ultrastructure of macrophage differentiation in the peritoneal cavity and in culture. J. Exp. Med. **123:**747–755.

17. **Connell, P., C. A. Ballinger, J. Jiang, Y. Wu, L. J. Thompson, J. Hohfeld, and C. Patterson.** 2001. The co-chaperone CHIP regulates protein triage decisions mediated by heat-shock proteins. Nat. Cell Biol. **3:**93–96.

18. **Czar, M. J., R. H. Lyons, M. J. Welsh, J. M. Renoir, and W. B. Pratt.** 1995. Evidence that the FK506-binding immunophilin heat shock protein 56 is required for trafficking of the glucocorticoid receptor from the cytoplasm to the nucleus. Mol. Endocrinol. **9:**1549–1560.

19. **Davies, B., L. S. Chattings, and S. W. Edwards.** 1991. Superoxide generation during phagocytosis by *Acanthamoeba castellanii*: similarities to the respiratory burst of immune phagocytes. J. Gen. Microbiol. **137:**705–710.

20. **Davies, B., and S. W. Edwards.** 1991. Chemiluminescence and superoxide production in *Acanthamoeba castellanii*: free radicals generated during oxidative stress. J. Gen. Microbiol. **137:**1021–1027.

21. **Denis, M., and J. A. Gustafsson.** 1989. The Mr approximately 90,000 heat shock protein: an important modulator of ligand and DNA-binding properties of the glucocorticoid receptor. Cancer Res. **49:**2275s–2281s.

22. **Edelstein, P. H.** 1981. Improved semiselective medium for isolation of *Legionella pneumophila* from contaminated clinical and environmental specimens. J. Clin. Microbiol. **14:**298–303.

23. **Engleberg, N. C., D. J. Drutz, and B. I. Eisenstein.** 1984. Cloning and expression of *Legionella pneumophila* antigens in *Escherichia coli*. Infect. Immun. **44:**222–227.

24. **Fliermans, C. B., W. B. Cherry, L. H. Orrison, S. J. Smith, D. L. Tison, and D. H. Pope.** 1981. Ecological distribution of *Legionella pneumophila*. Appl. Environ. Microbiol. **41:**9–16.

25. **Fliermans, C. B., W. B. Cherry, L. H. Orrison, and L. Thacker.** 1979. Isolation of *Legionella pneumophila* from nonepidemic-related aquatic habitats. Appl. Environ. Microbiol. **37:**1239–1242.

26. **Fujita, N., S. Sato, A. Ishida, and T. Tsuruo.** 2002. Involvement of Hsp90 in signaling and stability of 3-phosphoinositide-dependent kinase-1. J. Biol. Chem. **277:**10346–10353.

27. **Galigniana, M. D., C. Radanyi, J. M. Renoir, P. R. Housley, and W. B. Pratt.** 2001. Evidence that the peptidylprolyl isomerase domain of the hsp90-binding immunophilin FKBP52 is involved in both dynein interaction and glucocorticoid receptor movement to the nucleus. J. Biol. Chem. **276:**14884–14889.

28. **Garin, J., R. Diez, S. Kieffer, J. F. Dermine, S. Duclos, E. Gagnon, R. Sadoul, C. Rondeau, and M. Desjardins.** 2001. The phagosome proteome: insight into phagosome functions. J. Cell Biol. **152:**165–180.

29. **Grenert, J. P., W. P. Sullivan, P. Fadden, T. A. Haystead, J. Clark, E. Mimnaugh, H. Krutzsch, H. J. Ochel, T. W. Schulte, E. Sausville, L. M. Neckers, and D. O. Toft.** 1997. The amino-terminal domain of heat shock protein 90 (hsp90) that binds geldanamycin is an ATP/ADP switch domain that regulates hsp90 conformation. J. Biol. Chem. **272:**23843–23850.

30. **Hagele, S., R. Kohler, H. Merkert, M. Schleicher, J. Hacker, and M. Steinert.** 2000. Dictyostelium discoideum: a new host model system for intracellular pathogens of the genus Legionella. Cell Microbiol. **2:**165–171.

31. **Harlow, E. L. D.** 1988. Antibodies: a laboratory manual. Cold Spring Harbor Laboratory Press, Cold Spring Harbor, N.Y.

32. **Henke, M., and K. M. Seidel.** 1986. Association between *Legionella pneumophila* and amoebae in water. Isr. J. Med. Sci. **22:**690–695.

33. **Horwitz, M. A., and F. R. Maxfield.** 1984. Legionella pneumophila inhibits acidification of its phagosome in human monocytes. J. Cell Biol. **99:**1936–1943.

34. **Jin, S., Y. C. Song, A. Emili, P. M. Sherman, and V. L. Chan.** 2003. JlpA of Campylobacter jejuni interacts with surface-exposed heat shock protein 90α and triggers signalling pathways leading to the activation of NF-κB and p38 MAP kinase in epithelial cells. Cell Microbiol. **5:**165–174.

35. **Kaplan, G., W. C. Van Voorhis, E. N. Sarno, N. Nogueira, and Z. A. Cohn.** 1983. The cutaneous infiltrates of leprosy. A transmission electron microscopy study. J. Exp. Med. **158:**1145–1159.

36. **Koyasu, S., E. Nishida, T. Kadowaki, F. Matsuzaki, K. Iida, F. Harada, M. Kasuga, H. Sakai, and I. Yahara.** 1986. Two mammalian heat shock proteins, HSP90 and HSP100, are actin-binding proteins. Proc. Natl. Acad. Sci. USA **83:**8054–8058.

37. **Langer, T., H. Schlatter, and H. Fasold.** 2002. Evidence that the novobiocin-sensitive ATP-binding site of the heat shock protein 90 (hsp90) is necessary for its autophosphorylation. Cell Biol. Int. **26:**653–657.

38. **Lindquist, S., and E. A. Craig.** 1988. The heat-shock proteins. Annu. Rev. Genet. **22:**631–677.

39. **Lock, R., L. Öhman, and C. Dahlgren.** 1987. Phagocytic recognition mechanisms in human granulocytes and *Acanthamoeba castellanii* using type 1

fimbriated *Escherichia coli* as phagocytic prey. FEMS Microbiol. Lett. **44:**135–140.

40. **Marcu, M. G., A. Chadli, I. Bouhouche, M. Catelli, and L. M. Neckers.** 2000. The heat shock protein 90 antagonist novobiocin interacts with a previously unrecognized ATP-binding domain in the carboxyl terminus of the chaperone. J. Biol. Chem. **275:**37181–37186.

41. **Marcu, M. G., T. W. Schulte, and L. Neckers.** 2000. Novobiocin and related coumarins and depletion of heat shock protein 90-dependent signaling proteins. J. Natl. Cancer Inst. **92:**242–248.

42. **Moffat, J. F., P. H. Edelstein, D. P. Regula, Jr., J. D. Cirillo, and L. S. Tompkins.** 1994. Effects of an isogenic Zn-metalloprotease-deficient mutant of *Legionella pneumophila* in a guinea-pig model. Mol. Microbiol. **12:**693–705.

43. **Moffat, J. F., and L. S. Tompkins.** 1992. A quantitative model of intracellular growth of *Legionella pneumophila* in *Acanthamoeba castellanii*. Infect. Immun. **60:**296–301.

44. **Murphy, J. K., F. R. Livingston, E. Gozal, M. Torres, and H. J. Forman.** 1993. Stimulation of the rat alveolar macrophage respiratory burst by extracellular adenine nucleotides. Am. J. Respir. Cell Mol. Biol. **9:**505–510.

45. **Nakamura, T., J. Hinagata, T. Tanaka, T. Imanishi, Y. Wada, T. Kodama, and T. Doi.** 2002. HSP90, HSP70, and GAPDH directly interact with the cytoplasmic domain of macrophage scavenger receptors. Biochem. Biophys. Res. Commun. **290:**858–864.

46. **Neckers, L., T. W. Schulte, and E. Mimnaugh.** 1999. Geldanamycin as a potential anti-cancer agent: its molecular target and biochemical activity. Investig. New Drugs **17:**361–373.

47. **Neff, R. J.** 1957. Purification, axenic cultivation, and description of a soil amoeba, Acanthamoeba sp. J. Protozool. **4:**176–182.

48. **Nishida, E., S. Koyasu, H. Sakai, and I. Yahara.** 1986. Calmodulin-regulated binding of the 90-kDa heat shock protein to actin filaments. J. Biol. Chem. **261:**16033–16036.

49. **Niszl, I. A., and M. B. Markus.** 1989. Processing of free-living amoebae for transmission electron microscopy. Stain Tech. **64:**259–260.

50. **Oren, R., A. E. Farnham, K. Saito, E. Milofsky, and M. L. Karnovsky.** 1963. Metabolic patterns in three types of phagocytizing cells. J. Cell Biol. **17:**487–501.

51. **Panaretou, B., C. Prodromou, S. M. Roe, R. O'Brien, J. E. Ladbury, P. W. Piper, and L. H. Pearl.** 1998. ATP binding and hydrolysis are essential to the function of the Hsp90 molecular chaperone in vivo. EMBO J. **17:**4829–4836.

52. **Polesky, A. H., J. T. D. Ross, S. Falkow, and L. S. Tompkins.** 2001. Identification of *Legionella pneumophila* genes important for infection of amoebas by signature-tagged mutagenesis. Infect. Immun. **69:**977–987.

53. **Pratt, W. B., and D. O. Toft.** 2003. Regulation of signaling protein function and trafficking by the hsp90/hsp70-based chaperone machinery. Exp. Biol. Med. **228:**111–133.

54. **Prodromou, C., S. M. Roe, R. O'Brien, J. E. Ladbury, P. W. Piper, and L. H. Pearl.** 1997. Identification and structural characterization of the ATP/ADP-binding site in the Hsp90 molecular chaperone. Cell **90:**65–75.

55. **Ramakrishnan, L., and S. Falkow.** 1994. *Mycobacterium marinum* persists in cultured mammalian cells in a temperature-restricted fashion. Infect. Immun. **62:**3222–3229.

56. **Ramsby, M. L., G. S. Makowski, and E. A. Khairallah.** 1994. Differential detergent fractionation of isolated hepatocytes: biochemical, immunochemical and two-dimensional gel electrophoresis characterization of cytoskeletal and noncytoskeletal compartments. Electrophoresis **15:**265–277.

57. **Richter, K., and J. Buchner.** 2001. Hsp90: chaperoning signal transduction. J. Cell. Physiol. **188:**281–290.

58. **Roe, S. M., C. Prodromou, R. O'Brien, J. E. Ladbury, P. W. Piper, and L. H. Pearl.** 1999. Structural basis for inhibition of the Hsp90 molecular chaperone by the antitumor antibiotics radicicol and geldanamycin. J. Med. Chem. **42:**260–266.

59. **Rowbotham, T. J.** 1980. Preliminary report on the pathogenicity of *Legionella pneumophila* for freshwater and soil amoeba. J. Clin. Pathol. **33:**1179–1183.

60. **Schneider, C., L. Sepp-Lorenzino, E. Nimmesgern, O. Ouerfelli, S. Danishefsky, N. Rosen, and F. U. Hartl.** 1996. Pharmacologic shifting of a balance between protein refolding and degradation mediated by Hsp90. Proc. Natl. Acad. Sci. USA **93:**14536–14541.

61. **Sikora, A., J. Liu, C. Brosnan, G. Buell, I. Chessel, and B. R. Bloom.** 1999. Cutting edge: purinergic signaling regulates radical-mediated bacterial killing mechanisms in macrophages through a P2X7-independent mechanism. J. Immunol. **163:**558–561.

62. **Smith, D. F., L. Whitesell, S. C. Nair, S. Chen, V. Prapapanich, and R. A. Rimerman.** 1995. Progesterone receptor structure and function altered by geldanamycin, an hsp90-binding agent. Mol. Cell. Biol. **15:**6804–6812.

63. **Snapper, S. B., R. E. Melton, S. Mustafa, T. Kieser, and W. R. Jacobs, Jr.** 1990. Isolation and characterization of efficient plasmid transformation mutants of *Mycobacterium smegmatis*. Mol. Microbiol. **4:**1911–1919.

64. **Solomon, J. M., A. Rupper, J. A. Cardelli, and R. R. Isberg.** 2000. Intracellular growth of *Legionella pneumophila* in *Dictyostelium discoideum*, a system for genetic analysis of host-pathogen interactions. Infect. Immun. **68:**2939–2947.

65. **Sreedhar, A. S., K. Mihaly, B. Pato, T. Schnaider, A. Stetak, K. Kis-Petik, J.**

Fidy, T. Simonics, A. Maraz, and P. Csermely. 2003. Hsp90 inhibition accelerates cell lysis: anti-Hsp90 ribozyme reveals a complex mechanism of Hsp90 inhibitors involving both superoxide- and Hsp90-dependent events. J. Biol. Chem. **278:**35231–35240.

66. **Steenbergen, J. N., H. A. Shuman, and A. Casadevall.** 2001. Cryptococcus neoformans interactions with amoebae suggest an explanation for its virulence and intracellular pathogenic strategy in macrophages. Proc. Natl. Acad. Sci. USA **98:**15245–15250.

67. **Sussman, D. J., E. Y. Lai, and C. Fulton.** 1984. Rapid disappearance of translatable actin mRNA during cell differentiation in Naegleria. J. Biol. Chem. **259:**7355–7360.

68. **Tesic, M., J. A. Marsh, S. B. Cullinan, and R. F. Gaber.** 2003. Functional interactions between Hsp90 and the co-chaperones Cns1 and Cpr7 in Saccharomyces cerevisiae. J. Biol. Chem. **278:**32692–32701.

69. **Thom, S., D. Warhurst, and B. S. Drasar.** 1992. Association of *Vibrio cholerae* with fresh water amoebae. J. Med. Microbiol. **36:**303–306.

70. **Tonetti, M., L. Sturla, T. Bistolfi, U. Benatti, and A. De Flora.** 1994. Extra-cellular ATP potentiates nitric oxide synthase expression induced by lipopolysaccharide in RAW 264.7 murine macrophages. Biochem. Biophys. Res. Commun. **203:**430–435.

71. **Triantafilou, K., M. Triantafilou, S. Ladha, A. Mackie, R. L. Dedrick, N. Fernandez, and R. Cherry.** 2001. Fluorescence recovery after photobleaching reveals that LPS rapidly transfers from CD14 to hsp70 and hsp90 on the cell membrane. J. Cell Sci. **114:**2535–2545.

72. **Ward, B. K., R. K. Allan, D. Mok, S. E. Temple, P. Taylor, J. Dornan, P. J. Mark, D. J. Shaw, P. Kumar, M. D. Walkinshaw, and T. Ratajczak.** 2002. A structure-based mutational analysis of cyclophilin 40 identifies key residues in the core tetratricopeptide repeat domain that mediate binding to Hsp90. J. Biol. Chem. **277:**40799–40809.

73. **Weisman, R. A., and E. D. Korn.** 1967. Phagocytosis of latex beads by Acanthamoeba. I. Biochemical properties. Biochemistry **6:**485–497.

74. **Young, J. C., I. Moarefi, and F. U. Hartl.** 2001. Hsp90: a specialized but essential protein-folding tool. J. Cell Biol. **154:**267–273.